Journal of
Materials Chemistry

Cite this: *J. Mater. Chem.*, 2012, **22**, 8484

www.rsc.org/materials

PAPER

Stabilization of the blue phases of simple rodlike monoester compounds by addition of their achiral homologues†

Keiki Kishikawa,* Hiroyuki Itoh, Seiji Akiyama, Takahiro Kobayashi and Shigeo Kohmoto

Received 5th December 2011, Accepted 22nd February 2012
DOI: 10.1039/c2jm16359d

As novel rodlike liquid crystalline ester compounds exhibiting blue phases (*BP*s), chiral 4-(4′-alkoxyphenyl)phenyl 4-(4′-alkoxyphenyl)benzoate derivatives (R–C_6H_4–C_6H_4–OCO–C_6H_4–C_6H_4–R′), **1** (R = R′ = (*R*)-1-methylheptyloxy, *BP* range: 1.6 K on heating), **2** (R = (*R*)-1-methylheptyloxy, R′ = *n*-octyloxy, *BP* range: 0.8 K on heating), **4** (R = (*R*)-1-methylheptyloxy, R′ = H, *BP* range: 1.0 K on heating), were synthesized and their phase behaviors were investigated. Further, the *BP* of **1** was stabilized by addition of its achiral homologue ester compound **3** (R = R′ = *n*-octyloxy). In the range of the composite ratio of **1** : **3** from 10 : 0 to 0 : 10, the *BP* temperature range became wider with increase of the content of **3** in the mixture. At the ratio of 6 : 4, the *BP* indicated the widest temperature range in the mixing experiment (5.0 K on heating and 6.0 K on cooling).

Introduction

Cubic blue phases have unique superstructures in which rodlike molecules are organized into cylinder-like molecular aggregates with an internal helical alignment, “double twist cylinders” (Fig. 1a), and the cylinders are assembled into superstructures with cubic lattices (blue phases I and II (*BP*-Is and *BP*-IIs), Fig. 1b and c).[1] Their three-dimensionally periodical structures are useful for photonic devices such as tunable selective reflective devices,[2,3] and also for laser emitting devices.[4] However, the temperature ranges of *BP*s are so narrow (less than 1 K in most cases)[5] and expansion of them is so difficult that utilization of the phases for those optical devices is limited. Many scientists in the fields of chemistry, physics, and materials science have been challenging for realization of *BP*s with a wide temperature range. The reported methods are classified into (1) polymer-approaches and (2) low-molecular weight molecule approaches. As polymer-approaches, fixation of *BP*s by photopolymerization of doped monomers[6] and confining *BP*s in 3D polymer network structures[7] were reported. As low-molecular weight molecule approaches, liquid crystalline dimers possessing large flexoelectricity were used for stabilization of a *BP*-I, which realized the wide-temperature range of the *BP* only on cooling.[8] Further, chiral binaphthyl derivatives (*BP* range: 1.5 K on the first heating (two types of crystals exist in the pure sample) and about 30 K on the second heating–cooling cycle),[9] rodlike molecules connecting with cholesterol (*BP* range: 2.5 K),[10] and rodlike molecules possessing two asymmetric carbons (*BP* range: 2.5 K)[11] were reported, respectively. Recently, an enantiotropic cubic *BP* of a supramolecular compound with a wide temperature range (23 K) was reported by Yang's group,[12] and a cubic *BP* of an asymmetric dimer compound (*BP* ranges as the total range of *BP*I and *BP*II: about 9 K) was reported by Yelamaggad *et al.*[13] However, the mechanisms for the stabilization of those *BP* have not been clarified. Thus, the methodology for stabilization of cubic *BP*s in low-molecular weight molecule approaches has not been established yet, and expansion of the temperature range to more than 3 K on heating is still difficult.[14] In this paper, we describe synthesis of simple rodlike liquid crystalline monoester compounds exhibiting *BP*s (*BP* range: 0.8–1.6 K on heating) and stabilization of the *BP*s by

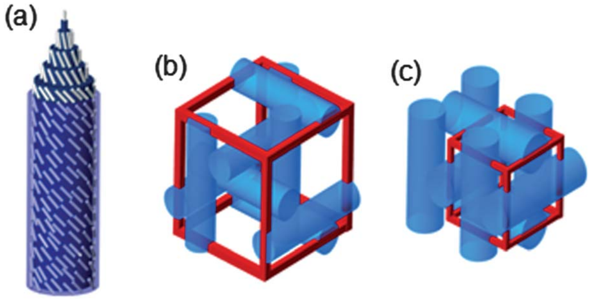

Fig. 1 Models of (a) “double twist cylinder” of *BP*s (a cylinder-like superstructure generated by helically aligned rodlike molecules), (b) unit cell of *BP*-I, and (c) unit cell of *BP*-II. The lattice units are indicated by red lines.

Department of Applied Chemistry and Biotechnology, Faculty of Engineering, Chiba University, 1-33 Yayoi-cho, Inage-ku, Chiba 263-8522, Japan. E-mail: kishikawa@faculty.chiba-u.jp; Fax: +81-43-290-3422; Tel: +81-43-290-3238

† Electronic supplementary information (ESI) available: Synthesis and spectral data of esters **1**, **2**, **3**, **4**, and **7**, and micro-photographs of **1**, **2**, a mixture of **1** and **3**, a mixture of **1** and **4**, and a mixture of **1** and **6**. Table of the temperature ranges of the *BP* in the mixtures of **1** and **3**. See DOI: 10.1039/c2jm16359d

addition of achiral homologues (the maximum *BP* range: 5.0 K on heating).

It is known that most *BP*s exist above chiral nematic phases exhibiting very short helical pitches (<5000 Å) and large helical twisting power is necessary to generate the helical superstructure from both theoretical and experimental studies.[15] Accordingly, addition of achiral molecules destabilizes *BP*s. However, as an exception, stabilization of *BP*s by addition of achiral bent rodlike compounds (1,3-phenylene bis[4-(4-octylphenyliminomethyl) benzoates] (P8PIMB) and racemic 4′-octyloxy-biphenyl-4-carboxylic acid 4-(1-methylheptyloxycarbonyl)phenyl ester (MHPOBC)) to a chiral nematic liquid crystal material (a 79 : 21 mixture of ZLI-2293 and MLC-6248) was reported by Takezoe's group (*BP* ranges as the total range of *BP*I, *BP*II, and amorphous *BP* (*BP*III)) for P8PIMB and MHPOBC: about 5 K and 4 K, respectively.[16] ZLI-2293 is a mixture of several nematic liquid crystal compounds and MLC-6248 is a chiral dopant compound, which are manufactured by Merck and the information on those molecular structures are not released. They concluded that the phenomena originated in the bent-type molecular shapes of P8PIMB and MHPOBC, because analogous sized straight rod molecules (terephthalylidene-bis-4-*n*-butylaniline (TBBA)) did not induce the *BP* under similar conditions. It is well known that achiral bent-core molecules show spontaneous chiral induction in the liquid crystal phases, and their explanation is understandable. However, stabilization of the *BP*s by addition of achiral rodlike molecules is hard to understand. To the best of our knowledge, it has not been reported yet.

In the double twist cylinders (Fig. 2), one molecule and each of the adjacent molecules are arranged twisted parallel. Though the chiral alkyl chains are effective for generation of the molecular arrangement, their steric repulsions suppress simultaneously the intermolecular attractive core–core interactions which are necessary for maintaining the superstructure in *BP*s. Accordingly, reduction of the intermolecular steric repulsion between their alkyl chains is effective for stabilization of *BP*s. Usually, partial replacement of the chiral molecules with their achiral homologues possessing less-bulky normal alkyl chains increases the intermolecular core–core attractive interactions. This also destabilizes the *BP*s because of decrease of the proportion of chiral molecules. However, our recent results showed that the addition of achiral ester compound **6** to a chiral nematic liquid crystalline compound enhanced the helicity in the chiral nematic phase.[17] It is explained that one chiral conformer of the achiral ester molecule is predominant over its mirror image under the chiral atmosphere, and the chiral ester conformer has larger twisting power than that of the original chiral liquid crystalline molecule. From these results, we prospected that (1) simple rodlike monoesters possessing chiral alkyl chains would generate strong helicity and exhibit *BP*s, and (2) addition of achiral rodlike esters to the chiral esters would increase the intermolecular attractive interactions without reducing their helicity, which stabilizes the *BP*.

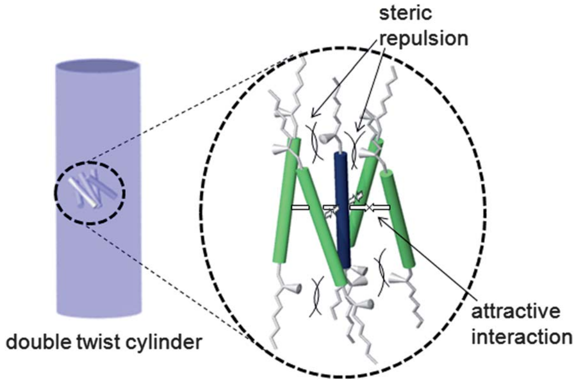

Fig. 2 Schematic representation of the arrangement of chiral molecules in the double twist cylinder. Each molecule interacts with the molecules surrounding it (the intermolecular attractive interactions and steric repulsions are indicated).

Results and discussion

Synthesis

We synthesized simple rodlike esters **1–5** (Scheme 1). These molecules were designed based on the molecular structure of **6**. The phenyl groups of **6** were replaced with biphenyl groups to make the intermolecular core–core interactions stronger.

Investigation of the phase transition behaviors of 1–5

The phase behaviors of **1–5** are shown in Table 1. Chiral compound **1** (R = R′ = (*R*)-1-methylheptyloxy) exhibited a *BP* with chiral smectic C and chiral nematic phases. The *BP* was observed in a narrow temperature range (1.6 K on heating). From the textures in POM (Fig. 3), the *BP*s observed in this study were identified as *BP*-Is.[18] Compound **2** (R = (*R*)-1-methylheptyloxy, R′ = *n*-octyloxy) exhibited a *BP* (Fig. 4) with 0.8 K on heating. Almost the same temperature range as that of **1** suggested that the effect of one chiral group in the molecule was the same as that of two chiral groups on temperature range of the *BP*. To investigate the additive effect of achiral rodlike ester molecules, the achiral homologue **3** (R = R′ = *n*-octyloxy) was

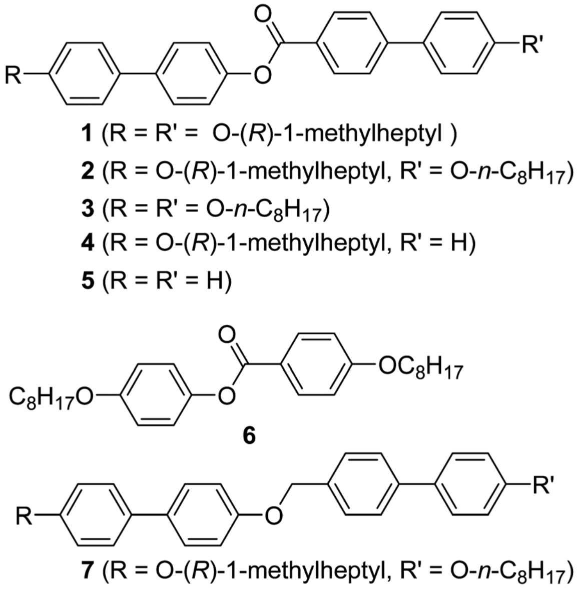

1 (R = R' = O-(*R*)-1-methylheptyl)
2 (R = O-(*R*)-1-methylheptyl, R' = O-*n*-C_8H_{17})
3 (R = R' = O-*n*-C_8H_{17})
4 (R = O-(*R*)-1-methylheptyl, R' = H)
5 (R = R' = H)
7 (R = O-(*R*)-1-methylheptyl, R' = O-*n*-C_8H_{17})

Scheme 1 Structures of **1–7**.

Table 1 Phase behaviours of **1–5** and **7**[a]

compound	phase transition (°C, (kcal/mol))
1	$\mathbf{Cr}\ \underset{89.2\ (-3.6)}{\overset{96.3\ (4.3)}{\rightleftarrows}}\ \mathbf{SmC^*}\ \underset{140.9\ (-0.37)}{\overset{141.5\ (0.35)}{\rightleftarrows}}\ \mathbf{N^*}\ \underset{165.1\ (\ -\ )^{b}}{\overset{166.1\ (\ -\ )^{b}}{\rightleftarrows}}\ \mathbf{BP}\ \underset{166.8\ (-0.13)}{\overset{167.7\ (0.12)}{\rightleftarrows}}\ \mathbf{Iso}$
2	$\mathbf{Cr1}\ \underset{94.7\ (-0.51)}{\overset{99.2\ (0.58)}{\rightleftarrows}}\ \mathbf{Cr2}\ \underset{122.1\ (-0.51)}{\overset{124.7\ (0.54)}{\rightleftarrows}}\ \mathbf{Cr3}\ \underset{136.9\ (-1.1)}{\overset{139.0\ (1.2)}{\rightleftarrows}}\ \mathbf{SmC^*}\ \underset{214.8(-0.09)}{\overset{218.4\ (0.06)}{\rightleftarrows}}\ \mathbf{SmA}$ $\underset{230.7\ (\ -\ )^{b}}{\overset{232.0\ (\ -\ )^{b}}{\rightleftarrows}}\ \mathbf{TGBA}\ \underset{231.9\ (-0.26)}{\overset{232.8\ (0.28)}{\rightleftarrows}}\ \mathbf{N^*}\ \underset{238.5\ (\ -\ )^{b}}{\overset{240.2\ (\ -\ )^{b}}{\rightleftarrows}}\ \mathbf{BP}\ \underset{240.1\ (-0.35)}{\overset{241.0\ (0.33)}{\rightleftarrows}}\ \mathbf{Iso}$
3	$\mathbf{Cr}\ \underset{145.5\ (-7.0)}{\overset{159.4\ (9.4)}{\rightleftarrows}}\ \mathbf{SmC}\ \underset{267.6\ (-0.13)}{\overset{269.4\ (0.14)}{\rightleftarrows}}\ \mathbf{N}\ \underset{292.7\ (-0.45)}{\overset{294.1\ (0.57)}{\rightleftarrows}}\ \mathbf{Iso}$
4	$\mathbf{Cr}\ \underset{155.7\ (-3.5)}{\overset{158.8\ (4.9)}{\rightleftarrows}}\ \mathbf{N^*}\ \underset{189.0\ (\ -\ )^{b}}{\overset{190.1\ (\ -\ )^{b}}{\rightleftarrows}}\ \mathbf{BP}\ \underset{190.7\ (-0.10)}{\overset{191.1\ (0.11)}{\rightleftarrows}}\ \mathbf{Iso}$
5	$\mathbf{Cr}\ \underset{212.8\ (-17.0)}{\overset{223.1\ (14.0)}{\rightleftarrows}}\ \mathbf{Iso}$
7	$\mathbf{Cr1}\ \underset{84.9\ (-2.7)}{\overset{106.5\ (2.7)}{\rightleftarrows}}\ \mathbf{Cr2}\ \underset{151.9\ (-0.45)}{\overset{157.5\ (0.60)}{\rightleftarrows}}\ \mathbf{SmC^*}\ \underset{196.2\ (h_3)^{c}}{\overset{200.7\ (h_1)^{c}}{\rightleftarrows}}\ \mathbf{N^*}\ \underset{201.4\ (h_4)^{c}}{\overset{205.5\ (h_2)^{c}}{\rightleftarrows}}\ \mathbf{Iso}$

[a] *SmC**, *SmC*, *N**, *N*, *BP*, *SmA*, *TGBA*, and *Iso* indicate chiral smectic C, smectic C, chiral nematic, nematic, blue, smectic A, twist grain boundary A, and isotropic liquid phases, respectively. *Cr*, *Cr*1, *Cr*2, and *Cr*3 indicate crystal phases. The heating and cooling rates are 5 °C min^{-1}. The transition temperature (°C) is indicated above and below the arrows, and each transition enthalpy (kcal mol^{-1}) is written in the parenthesis. [b] The transition temperature was measured by POM. [c] $h_1 + h_2 = 2.1$ and $h_3 + h_4 = -1.9$.

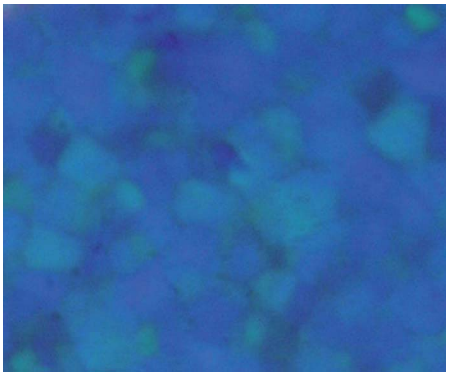

Fig. 3 Microphotograph of **1** on cooling (blue phase, 600×, 150.5 °C).

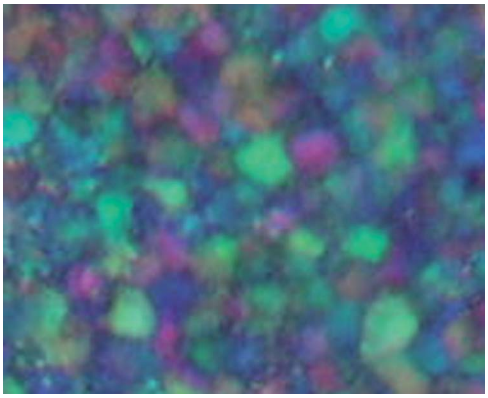

Fig. 4 Microphotograph of **2** on cooling (blue phase, 600×, 239.0 °C).

prepared. Compound **3** showed smectic C and nematic phases, whose transition temperatures (*SmC–N* and *N–Iso*) were higher than those of **1** and **2**, respectively. It was assumed that the replacement of the chiral alkyl chains with the normal alkyl chains reduced the intermolecular steric repulsions and increased the intermolecular attractive interactions, which caused the significant increase in the melting and clearing points.

Mixing experiments of 1 with 3–6

The phase diagram of the mixture of **1** and **3** against the mole fraction of **3** in **1** ($= x_3$) is shown in Fig. 5a and b. With an increase of x_3, the transition temperatures are increased except that of *SmC–N* phases. At $x_3 = 0.4$ and 0.5, the transition temperatures of *SmC–N* are higher than those at $x_3 = 0.6$ and 0.7. Temperature ranges of *BP* of the mixtures are shown in Fig. 6. At $x_3 = 0.0$–0.4, the temperature range of the *BP* becomes wider with an increase of the content of **3** in the mixture. At $x_3 = 0.4$, the *BP* indicated the widest temperature range (5.0 and 6.0 K on heating and cooling, respectively) in this mixing experiment and the textures in POM at $x_3 = 0.4$–0.5 were observed as clear and large mosaic patterns (Fig. 7). However, at $x_3 = 0.5$–0.7, the temperature range becomes narrow with increase of the content of **3**. At $x_3 = 0.8$ and 0.9, the *BP* is not observed. The phase transition behavior at $x_3 =$ 0.4 (**1** : **3** = 6 : 4) is shown in entry 1 of Table 2. The transition temperatures of the *N–BP* and *BP–Iso* were much higher than those of pure **1**, which meant that the intermolecular interactions became larger by addition of **3**. It strongly suggests that the intermolecular interaction is important to keep the wide

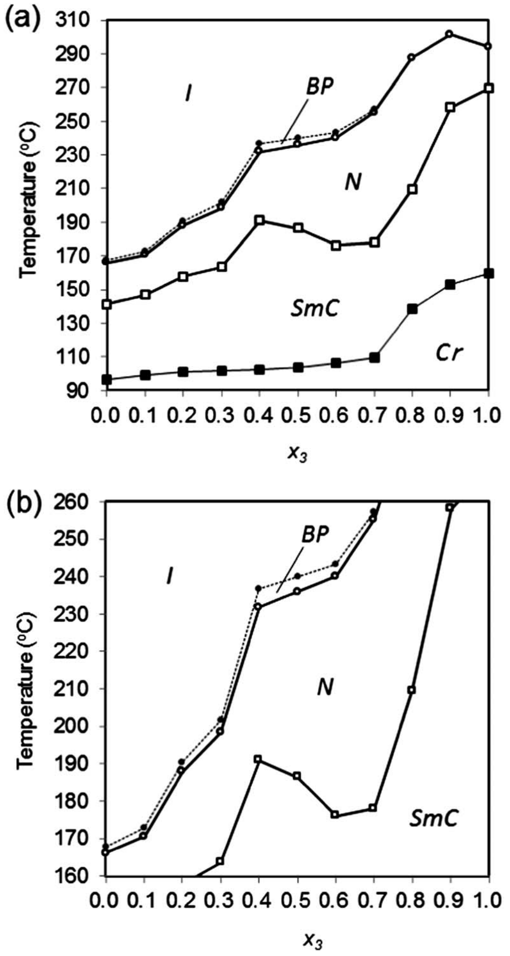

Fig. 5 Phase diagram (a) and its magnified one (b) in the mixtures of **1** and **3**. The mole fraction of **3** in **1** is indicated by x_3. *Cr*, *SmC*, *N*, *BP* and *Iso* indicate crystal, smectic C, nematic, blue and isotropic liquid phases, respectively. The transition temperatures were measured by POM with a temperature rate of 0.1 °C min^{-1}.

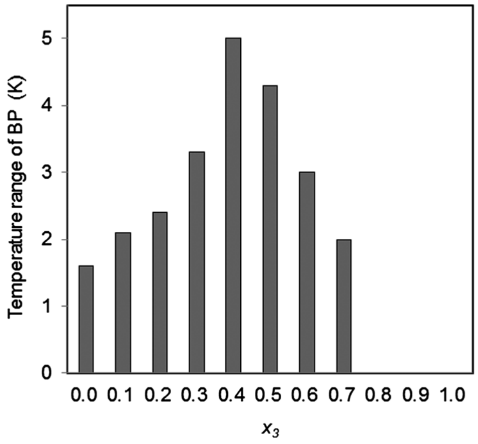

Fig. 6 Temperature ranges of the *BP* of the mixtures of **1** : **3**. The mole fraction of **3** in **1** is indicated by x_3.

temperature range of the *BP*. This experiment also indicates that addition of more than one equivalent of **3** to **1** destabilizes the *BP*.

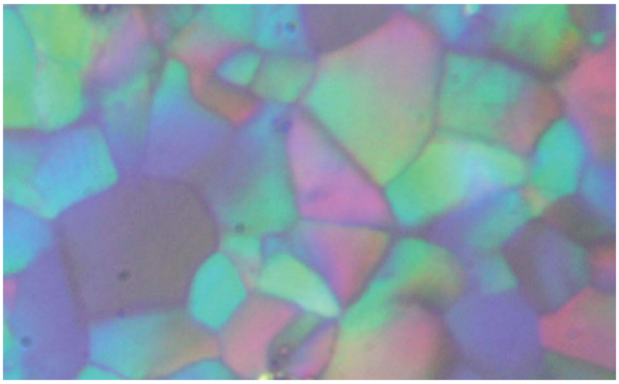

Fig. 7 Microphotograph of the mixture of **1** and **3** at the ratio of 5 : 5 ($x_3 = 0.5$) on cooling (600×, 227.5 °C).

In order to reduce the intermolecular steric repulsions, compound **1** was mixed with **4** and **5**, respectively. Compound **4** (R = (*R*)-1-methylheptyloxy, R′ = H) possesses the chiral chain at one terminal and no chain at the other terminal, and **5** (R = R′ = H) does not possess any terminal chain. The temperature ranges of the *BP* of the mixture of **1** and **4** (= 5 : 5) were 1.9 and 2.2 K on heating and cooling, respectively (entry 2 of Table 2). The temperature range of the *BP* increased slightly. In the mixture of **1** and **5** with the ratio of 5 : 5, crystals of **5** were segregated partially from the mixture in the liquid crystal phase. To avoid this, the mixture of **1** and **5** with the ratio of 8 : 2 was prepared. It was homogeneous in both liquid crystal and isotropic liquid phases (entry 3 of Table 2). Its temperature ranges of the *BP* on heating and cooling were 2.3 and 2.9 K, respectively. The effects of **4** and **5** on the expansion of the *BP* range were smaller than that of **3**.

In order to investigate matching in the core lengths of chiral and achiral molecules, compound **1** was mixed with **6** in the ratio of 5 : 5 (entry 4 of Table 2). The temperature ranges of the *BP* on heating and cooling were 1.0 and 1.5 K, respectively. The mixing of achiral and chiral molecules with different core lengths was not effective for stabilization of the *BP*. Further, the phase diagram of the mixture of **1** and **6** against the mole fraction of **6** in **1** (= x_6) was investigated (Fig. 8a and b). With increase of x_6, each of the transition temperatures, *BP–Iso*, *N–BP*, and *SmC–N*, decreased. Temperature ranges of the *BP* are shown in Fig. 9. At $x_6 = 0.0$, the *BP* indicated the widest temperature range (1.7 K on heating) in this mixing experiment. At x_6 = 0.0–0.6, the temperature range of the *BP* becomes narrower with increase of the content of **6** in the mixture, and at $x_6 > 0.7$, the *BP* is not observed. The textures at $x_6 = 0.5$ were observed as small mosaic patterns (Fig. 10). The phase diagram also suggests that mixing of the achiral and chiral molecules with different core lengths decreases the transition temperatures and narrows the *BP* temperature range.

Investigation of the selective reflection and helical twisting powers of the mixtures of 1 with 3 and 6

The selective reflections of the pure chiral compound **1** and the mixtures of **1** and **3** were carried out by POM at $T - T_{BP\text{–}N} = 5$ K ($T_{BP\text{–}N}$: transition temperature between the *BP* and nematic

Table 2 Phase transitions of the mixtures of **1** with **3**, **4**, **5**, and **6**[a]

entry	Compound (ratio)	phase transition (°C)
1	**1+3** (6:4)	**Cr** $\underset{94.0}{\overset{102.3}{\rightleftarrows}}$ **SmC*** $\underset{189.5}{\overset{190.9}{\rightleftarrows}}$ **N*** $\underset{230.3}{\overset{231.8}{\rightleftarrows}}$ **BP** $\underset{236.3}{\overset{236.8}{\rightleftarrows}}$ **Iso**
2	**1+4** (5:5)	**Cr** $\underset{95.3}{\overset{99.2}{\rightleftarrows}}$ **SmC*** $\underset{140.7}{\overset{141.4}{\rightleftarrows}}$ **SmA*** $\underset{158.1}{\overset{158.5}{\rightleftarrows}}$ **TGBA** $\underset{158.6}{\overset{159.5}{\rightleftarrows}}$ **N*** $\underset{184.1}{\overset{184.6}{\rightleftarrows}}$ **BP** $\underset{186.3}{\overset{186.5}{\rightleftarrows}}$ **Iso**
3	**1+5** (8:2)	**Cr** $\underset{120.8}{\overset{146.9}{\rightleftarrows}}$ **SmA*** $\underset{152.1}{\overset{152.8}{\rightleftarrows}}$ **TGBA** $\underset{153.9}{\overset{156.1}{\rightleftarrows}}$ **N*** $\underset{185.5}{\overset{186.4}{\rightleftarrows}}$ **BP** $\underset{188.4}{\overset{188.7}{\rightleftarrows}}$ **Iso**
4	**1+6** (5:5)	**Cr** $\underset{-0.5}{\overset{37.0}{\rightleftarrows}}$ **SmC*** $\underset{96.0}{\overset{97.6}{\rightleftarrows}}$ **N*** $\underset{121.4}{\overset{122.6}{\rightleftarrows}}$ **BP** $\underset{122.9}{\overset{123.6}{\rightleftarrows}}$ **Iso**

[a] *Cr*, *SmC**, *N**, *BP*, *SmA**, *TGBA*, and *Iso* indicate crystal, chiral smectic C, chiral nematic, blue, chiral smectic A, twist grain boundary A, and isotropic liquid phases, respectively. The transition temperature (°C) is indicated above and below the arrows. The transition temperature was measured by POM with a temperature rate of 0.1 °C min^{-1}.

phase) without the polarizers. Pure chiral compound **1** did not have color. The mixtures at 9 : 1 and 8 : 2 showed orange-red and green-yellow, which was surprising because this meant that the helical pitch became shorter by addition of achiral compound **3**. Choi *et al.* also reported this chiral enhancement in the addition of achiral compound **6** to a chiral nematic liquid crystalline compound.[17] Accordingly, it is assumed that the decrease of the helical pitch is common to these rodlike LC ester compounds (**3** and **6**). However, the mixtures at 7 : 3 and 6 : 4 showed orange and orange-red, and at 5 : 5 it exhibited pale red, which meant that the helical pitch became longer by addition of the achiral compound (**3**). It is usual that the helical pitch increases with a decrease of the proportion of chiral molecules. From these investigations, it is assumed that the chiral enhancement occurs only in high-concentrated mixture of **1** in **3**.

To investigate the correlation between the helical twisting powers (HTPs) and the width of the temperature ranges of the *BP*s, the HTPs of the mixtures **1**·**3** and **1**·**6** were measured by the Cano wedge method. The HTPs of the mixtures **1**·**3** (10 : 90) and **1**·**6** (5 : 95) were 8.1 and 12.9 μm^{-1} at $T_{N\text{–}Iso} - T = 5$ K (275.5 and 87.1 °C), respectively. The order of the HTPs in **1**·**3** and **1**·**6** did not agree with the widths of the temperature ranges of the *BP*s. This result indicates that compounds with a higher HTP do not necessarily give wider *BP* temperature ranges.

Investigation of the effect of the carbonyl group in compound 2 on the stabilization of the *BP*

To investigate the importance of the ester group, we prepared compound **7** possessing a –CH$_2$O– group instead of the ester group (–(C=O)–O–) in **2**. The phase behavior of **7** is shown in Table 1. In POM, **7** did not exhibit any *BP*, and showed clear finger print textures (5 μm at $T_{N\text{–}Iso} - T = 5$ K) in its chiral nematic phase, which meant that its helical pitch was much longer than that of **2**. In the POM of **2**, the finger print textures were not observed because of the very short helical pitches in its chiral nematic phase. Accordingly, it was confirmed that the ester group played an important role in generating the strong helicity in these chiral liquid crystal phases. The twisted molecular conformation and/or the dipole of the ester moiety are thought to be the important factors for generation of the short helical pitches.

Mechanism estimated for stabilization of the *BP* by addition of achiral compounds

We postulate the following mechanism for stabilization of the *BP* of **1** by addition of its achiral homologues. The ester molecules (**1**) in the *BP* cancel out their dipoles by generation of time-averaged anti-parallel dimers, in which the two rodlike molecules are arranged twisted parallel (Fig. 11a). It is assumed that an introduction of the chiral terminal chain affects the handedness (right- or left-handedness) in the arrangement of the two rodlike molecules and the induced handedness strongly influences the conformation of chirally twisted ester group (Fig. 12).[17] In the case of **1**, the chiral bulky chains in the dimers (homodimers **1**·**1**) cause large steric repulsions between the two molecules (Fig. 11a). On the other hand, in the case of the heterodimer **1**·**3** (Fig. 11b), the intermolecular steric repulsions are smaller than those of **1**·**1**, and the intermolecular attractive interactions of **1**·**3** are stronger than those of **1**·**1**. In the case of **1**·**3**, it is assumed that both ester groups of **1** and **3** have the same chiral conformation to stabilize the complexation as shown in Fig. 13, in which attractive electrostatic interaction between the two ester groups and π–π interactions between the benzene rings interact effectively. However, at the ratio exceeding **1** : **3** = 6 : 4, the *BP* was destabilized because of the decrease in the ratio of the chiral molecules in the environment. Accordingly, the temperature

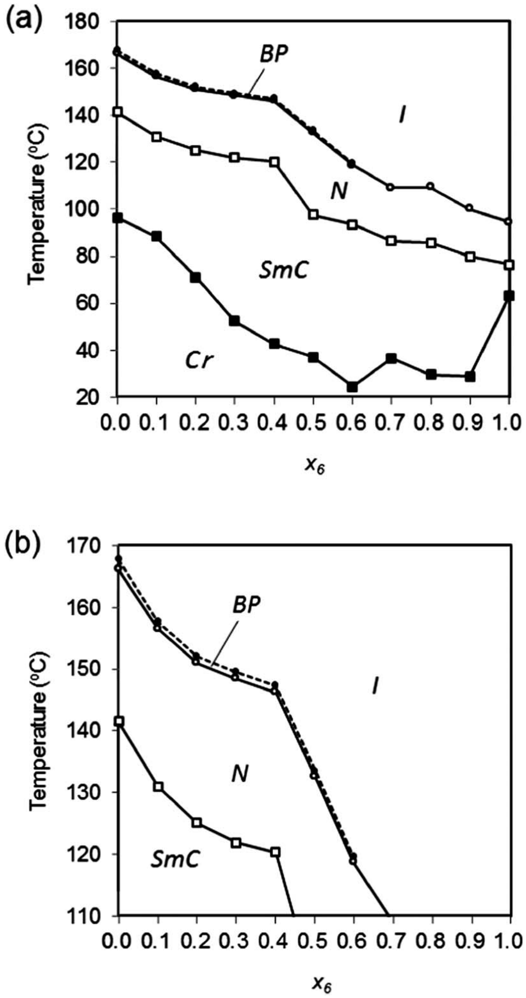

Fig. 8 Phase diagram (a) and its magnified one (b) in the mixtures of **1** and **6**. The mole fraction of **6** in **1** is indicated with x_6. *Cr*, *SmC*, *N*, *BP* and *Iso* indicate crystal, smectic C, smectic A, nematic, blue and isotropic liquid phases, respectively. The transition temperatures were measured by POM with a temperature rate of 0.1 °C min^{-1}.

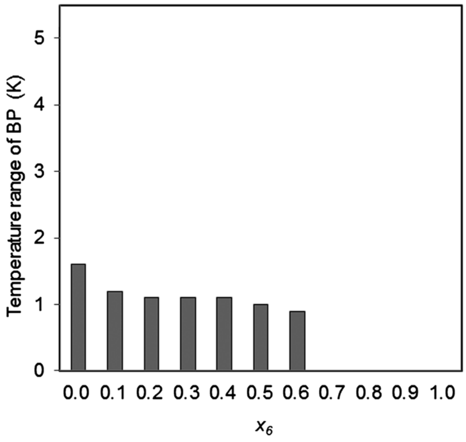

Fig. 9 Temperature ranges of the *BP* of the mixtures of **1** : **6**. The mole fraction of **6** in **1** is indicated by x_6.

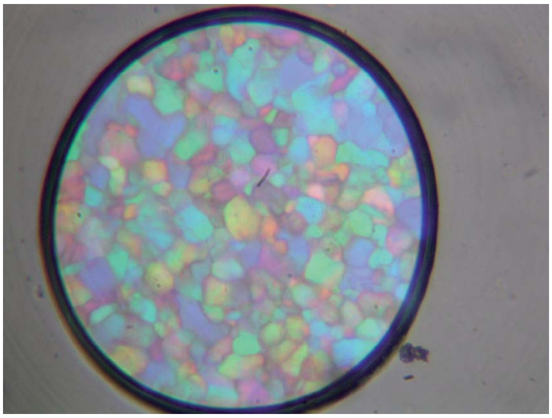

Fig. 10 Microphotograph of the mixture of **1** and **6** at the ratio of 5 : 5 (x_6 = 0.5) on cooling (600×, 125.0 °C).

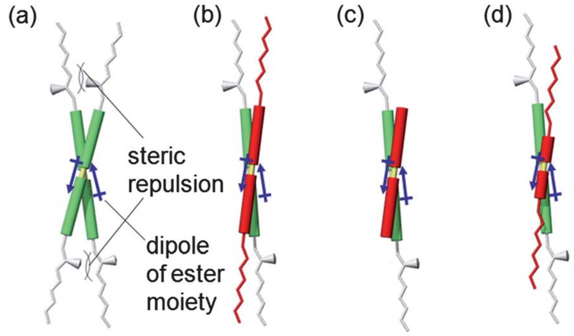

Fig. 11 Schematic representation of time-averaged dimers generated by intermolecular dipole–dipole interaction; (a) homodimer of two chiral rodlike molecules (**1·1**), (b) heterodimer of chiral and achiral rodlike molecules (**1·3**) (no difference in their core lengths), (c) heterodimer of chiral rodlike molecule and achiral non-alkylated rodlike molecule (**1·5**), and (d) heterodimer of chiral and achiral rodlike molecules (**1·6**) (difference in their core lengths).

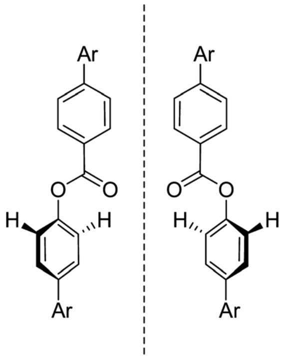

Fig. 12 The racemic pair of the chirally twisted conformations of **1** (Ar = 4-((*R*)-1-methylheptyloxy)phenyl).

range of the *BP* against the content ratio of **3**/(**1** + **3**) should have the local maximum. The mixing experiment of **1** with **4**, and **1** with **5**, showed that the terminal alkyl chains were necessary for expansion of the *BP* temperature range (Fig. 11c). In addition, the mixing experiment of **1** with **6** indicated the importance of matching in their core lengths to expand the *BP* temperature

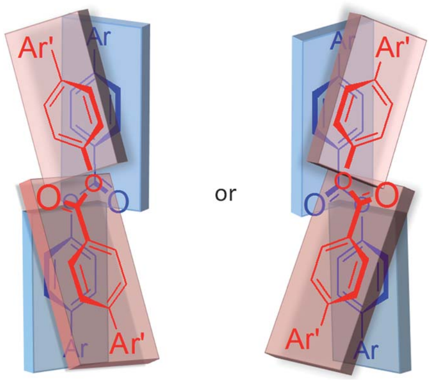

Fig. 13 The estimated models for the time-averaged anti-parallel heterodimer **1**·**3** (molecules **1** and **3** are indicated in blue and red, respectively. Ar = 4-((*R*)-1-methylheptyloxy)phenyl, Ar′ = 4-octyloxyphenyl) generated by π–π interactions and attractive electrostatic interactions. Both molecules in each dimer have the same chirality in their twisted ester-conformations.

range. Because of the difference in their core lengths, the anti-parallel heterodimer **1**·**6** (Fig. 11d) cannot have enough intermolecular attractive interactions.

By addition of **3** to **1** up to **1** : **3** = 6 : 4, an increment in the *BP*-I transition temperature was larger than that in the *N**–*BP* transition temperature, which resulted in the expansion of temperature range of the *BP*. This phenomenon is explained as follows. The achiral rodlike molecule **3** is sterically less-hindered than the chiral molecule **1**. Accordingly, in the *BP* of the mixture of **1** and **3**, the molecule **3** interacts equally with each of the laterally surrounded **1**, which stabilizes the superstructure "double twist cylinder" of the *BP*. In contrast, in chiral nematic phases molecules are aligned one-directionally in each of planes and the planes stack in parallel with changing the directors helically. The laterally omnidirectional interaction of molecule **3** with its adjacent molecules generates the heterodimers **1**·**3** even within the same plane, which destabilizes the one-dimensionally helical superstructure of the chiral nematic phase.

Conclusions

We realized a *BP* by using simple rodlike monoester compounds possessing asymmetric carbons and demonstrated that cubic *BP*s of a chiral ester compound could be stabilized by addition of its achiral homologue ester compound. This study suggested that increase of the intermolecular attractive forces is important for stabilization of *BP*s. We believe that this methodology is also useful to stabilize *BP*s of other rodlike liquid crystalline ester compounds. Further, in the mixing of the chiral molecules and the several achiral homologues, we also found that existence of the terminal alkyl chains and matching in the core lengths are important for stabilization of the *BP*. The information obtained in these results should also be important for designing the molecules exhibiting stable *BP*s.

Recently, it is reported that the stability of *BP*s is related to their elastic constants, especially the ratio K_{33}/K_{11} is known as one of the important factors (K_{33}, K_{11}: elastic constants for bend and splay transformations, respectively). However, some reports conclude that smaller K_{33}/K_{11} stabilizes *BP*s,[19,20] while the other describes that larger K_{33}/K_{11} stabilizes *BP*s.[21] The relationship between the ratio and stability of the *BP*s is not fully clarified. Though we did not approach the *BP* stability from the elastic constants in this study, we would like to measure the constants of the mixtures of **1** and **3** as our next project.

Acknowledgements

We are grateful to Mukai Science and Technology Foundation, the Asahi Glass Foundation for the funds, and we thank Grant-in-Aid for Scientific Research (B) 19350090.

Notes and references

1 H. Stegemeyer, T. Blümel, K. Hiltrop, H. Onusseit and F. Porsch, *Liq. Cryst.*, 1986, **1**, 3; Phase Structures and Transitions in Thermotropic Liquid Crystals, in *Handbook of Liquid Crystal Research*, ed. P. J. Collings and J. S. Patel, Oxford University Press, New York, 1997, ch. 4, pp. 106–108; Phase Transitions, Barois, in *Physical Properties of Liquid Crystals*, ed. D. Demus, J. Goodby, G. W. Gray, H.-W. Spiess and V. Vill, Wiley-VCH, New York, 1999, ch. 6, pp. 223–224; S. Hekimoglu and J. Conn, *Liq. Cryst. Today*, 2003, **12**, 1; Defect Structures, in *One and Two-Dimensional Fluids—Properties of Smectic, Lamellar and Columnar Liquid Crystals*, ed. A. Jakli and S. Saupe, Taylor and Francis, New York, 2006, ch. 6, pp. 199–201; K. Higashiguchi, K. Yasui and H. Kikuchi, *J. Am. Chem. Soc.*, 2008, **130**, 6326.

2 P. R. Gerber, *Mol. Cryst. Liq. Cryst.*, 1985, **116**, 197; H. J. Coles and H. F. Gleeson, *Mol. Cryst. Liq. Cryst.*, 1989, **167**, 213; V. E. Dmitrienko, *Liq. Cryst.*, 1989, **5**, 847; H.-S. Kitzerow, *Mol. Cryst. Liq. Cryst.*, 1991, **202**, 51; G. Heppke, B. Jerome, H.-S. Kitzerow and P. Pieranski, *J. Phys.*, 1991, **50**, 2291; P. Etchegoin, *Phys. Rev. E: Stat. Phys., Plasmas, Fluids, Relat. Interdiscip. Top.*, 2000, **62**, 1435.

3 Y. Hisakado, H. Kikuchi, T. Nagamura and T. Kajiyama, *Adv. Mater.*, 2005, **17**, 96; M. Sato and A. Yoshizawa, *Adv. Mater.*, 2007, **19**, 4145.

4 W. Cao, A. Muñoz, P. Palffy-Muhoray and B. Taheri, *Nat. Mater.*, 2002, **1**, 111; S. Yokoyama, S. Mashiko, H. Kikuchi, K. Uchida and T. Nagamura, *Adv. Mater.*, 2006, **18**, 48.

5 H.-S. Kitzerow, *ChemPhysChem*, 2006, **7**, 63.

6 H.-S. Kitzerow, H. Schmid, A. Ranft, G. Heppke, R. A. M. Hikmet and J. Lub, *Liq. Cryst.*, 1993, **14**, 911; H. Kikuchi, M. Yokota, Y. Hisakado, H. Yang and T. Kajiyama, *Nat. Mater.*, 2002, **1**, 64.

7 T. Noma, M. Ojima, H. Asagi, Y. Kawahira, A. Fujii, M. Ozaki and H. Kikuchi, *e-J. Surf. Sci. Nanotechnol.*, 2008, **6**, 17.

8 H. J. Coles and M. N. Pivnenko, *Nature*, 2005, **436**, 997.

9 A. Yoshizawa, Y. Kogawa, K. Kobayashi, Y. Takanishi and J. Yamamoto, *J. Mater. Chem.*, 2009, **19**, 5759.

10 C. V. Yelamaggad, N. L. Bonde, A. S. Achalkumar, D. S. S. Rao, S. K. Prasad and A. K. Prajapati, *Chem. Mater.*, 2007, **19**, 2463.

11 S.-L. Wu and W.-J. Hsieh, *Chem. Mater.*, 2003, **15**, 4515.

12 W. He, G. Pan, Z. Yang, D. Zhao, G. Niu, W. Huang, X. Yuan, J. Guo, H. Cao and H. Yang, *Adv. Mater.*, 2009, **21**, 2050.

13 C. V. Yelamaggad, V. P. Tamilenthi, D. Shankar Rao, G. G. Nair and S. Krishna Prasad, *J. Mater. Chem.*, 2009, **19**, 2906.

14 Examples of cubic *BP*s recently reported: T. Seshadri and H.-J. Haupt, *Chem. Commun.*, 1998, 735; J. Buey, P. Espinet, H.-S. Kitzerow and J. Strauss, *Chem. Commun.*, 1999, 441; R. Bayón, S. Coco and P. Espinet, *Chem. Mater.*, 2002, **14**, 3515; W.-R. Chen and J.-C. Hwang, *Liq. Cryst.*, 2004, **31**, 1539; J. Rokunohe and A. Yoshizawa, *J. Mater. Chem.*, 2005, **15**, 275; M. L. Parra, P. I. Hidalgo and E. Y. Elgueta, *Liq. Cryst.*, 2008, **35**, 823; J.-S. Hu, K.-Q. Wei, B.-Y. Zhang and L.-Q. Yang, *Liq. Cryst.*, 2008, **35**, 925; M. L. Parra, P. I. Hidalgo, E. A. Soto-Bustamante, J. Barberá, E. Y. Elgueta and V. H. Trujillo-Rojo, *Liq. Cryst.*, 2008, **35**, 1251; Y. Kogawa and A. Yoshizawa, *Liq. Cryst.*, 2011, **38**, 303.

15 H. Grebel, R. M. Hornreich and S. Shtrikman, *Phys. Rev. A: At., Mol., Opt. Phys.*, 1983, **28**, 1114; M. B. Bowling, P. J. Collings,

C. J. Booth and J. W. Goodby, *Phys. Rev. E: Stat. Phys., Plasmas, Fluids, Relat. Interdiscip. Top.*, 1993, **48**, 4113.

16 M. Nakata, Y. Takanishi, J. Watanabe and H. Takezoe, *Phys. Rev. E: Stat. Phys., Plasmas, Fluids, Relat. Interdiscip. Top.*, 2003, **68**, 041710.

17 S.-W. Choi, K. Fukuda, S. Nakahara, K. Kishikawa, Y. Takanishi, K. Ishikawa, J. Watanabe and H. Takezoe, *Chem. Lett.*, 2006, **35**, 896; S. Kawauchi, S.-W. Choi, K. Fukuda, K. Kishikawa, J. Watanabe and H. Takezoe, *Chem. Lett.*, 2007, **36**, 750.

18 The colors and shapes of the platelets were compared with *BP*-Is in the previous papers (for example; ref. 6, 8 and 16).

19 G. P. Alexander and J. M. Yeomans, *Phys. Rev. E: Stat., Nonlinear, Soft Matter Phys.*, 2006, **74**, 061706.

20 S.-T. Hur, M.-J. Gima, H.-J. Yoo, S.-W. Choi and H. Takezoe, *Soft Matter*, 2011, **7**, 8800.

21 S.-K. Hong, H. S. Choi, S. Shibayama, H. Higuchi and H. Kikuchi, *Mol. Cryst. Liq. Cryst.*, 2010, **528**, 32.